Enabling Precision Agriculture Through Embedded Sensing With Artificial Intelligence

Machine learning & Artificial Intelligence (Indian Institute of Technology (Indian School of Mines), Dhanbad)

Enabling Precision Agriculture Through Embedded Sensing With Artificial Intelligence

Dmitrii Shadrin, Alexander Menshchikov, Andrey Somov, Gerhild Bornemann, Jens Hauslage, and Maxim Fedorov

***Abstract*— Artificial intelligence (AI) has smoothly penetrated in a number of monitoring and control applications including agriculture. However, research efforts toward low-power sensing devices with fully functional AI on board are still fragmented. In this article, we present an embedded system enriched with the AI, ensuring the continuous analysis and *in situ* prediction of the growth dynamics of plant leaves. The embedded solution is grounded on a low-power embedded sensing system with a graphics processing unit (GPU) and is able to run the neural network-based AI on board. We use a recurrent neural network (RNN) called the long short-term memory network (LSTM) as a core of AI in our system. The proposed approach guarantees the system autonomous operation for 180 days using a standard Li-ion battery. We rely on the state-of-the-art mobile graphical chips for "smart" analysis and control of autonomous devices. This pilot study opens up wide vista for a variety of intelligent monitoring applications, especially in the agriculture domain. In addition, we share with the research community the Tomato Growth data set.**

***Index Terms*— Artificial intelligence (AI), embedded sensing, precision agriculture, sensing and control, smart sensing.**

I. Introduction

A NUMBER of remote areas, as well as developing countries, keep facing the problem of food production and provisioning. Indeed, the societal concerns regarding the environmental impact and food safety have generated the growing interest to the state-of-the-art technologies, which are supposed to help in this context [1], [2]. Precision agriculture is a technological paradigm that aims at optimizing the observation of outcomes of an agricultural system by automatizing observing, measuring, and responding stages while keeping the overall control of the system efficient in terms of resources. The precision agriculture, indeed, opens up a wide perspective for the usage of the state-of-the-art technologies that have been successfully applied recently, e.g., remote sensing [3], artificial intelligence (AI) [4], robotics [5], sensor networks [6], and Internet of Things (IoT) [7]. These technologies are promising in terms of securing the food safety, reducing the negative anthropogenic impact on the environment, and, finally, ensuring profit for the economy.

In spite of the great progress made in the precision agriculture in recent years, some challenges remain unresolved. Indeed, a high number of approaches have already been proposed to automate greenhouses and process environmental data [8], [9]. However, the problem of automating greenhouses and monitoring of plant growth in remote areas (particularly in developing countries) [10] still exists. This can be explained by the challenges associated with the system autonomous operation and transmission of collected data to high-performance computers/clouds for further processing. In terms of autonomous operation, it is the limited energy storage and high-power consumption that have been of great concern.

Regarding prediction, there is a lack of robust universal models available for the quantitative description of plant biomass changing with time that are able to perform the predictive analysis. Although there are mathematical models that can be applied to direct the simulation of plant growth (the so-called "bottom-up" approach [11]), most of them are based on solving systems of differential equations and involve large numbers of (semi) empirical parameters. Therefore, they have to be adapted to each specific type of plants, as well as to the cultivation technique. This makes them sensitive to some hidden changes in the environmental and other conditions that are difficult to track [12]. In fact, technically, in the remote areas, it is almost impossible to obtain all the necessary parameters for making a good quality predictive model to assess the plant growth dynamics based on the "bottom-up" approach.

To address the above problem, a distributed low-power embedded solution with AI on board is required. This solution is in line with the "edge computing" paradigm aimed at data processing with the AI on board the sensing device without involving complicated data transmission and its further processing in the cloud.

In this article, we report on the development of the low-power embedded system enriched with the AI based on a recurrent neural network (RNN) [13]. The proposed solution is capable of collecting the relevant agricultural data and performing the *in situ* prediction of the leave growth dynamics.

Manuscript received March 11, 2019; revised September 5, 2019; accepted September 23, 2019. Date of publication October 14, 2019; date of current version June 9, 2020. The Associate Editor coordinating the review process was V. R. Singh. *(Corresponding author: Alexander Menshchikov.)*

D. Shadrin, A. Menshchikov, A. Somov, and M. Fedorov were with the Center for Computational and Data-Intensive Science and Engineering (CDISE), Skolkovo Institute of Science and Technology, 121205 Moscow, Russia (e-mail: dmitry.shadrin@skolkovotech.ru; alexander.menshchikov@skolkovotech.ru; a.somov@skoltech.ru; m.fedorov@skoltech.ru).

G. Bornemann and J. Hauslage are with the DLR Institute of Aerospace Medicine, 51147 Cologne, Germany (e-mail: gerhild.bornemann@dlr.de; jens.hauslage@dlr.de).

Color versions of one or more of the figures in this article are available online at http://ieeexplore.ieee.org.

Digital Object Identifier 10.1109/TIM.2019.2947125

This approach features the system autonomous operation and is assessed on an experimental testbed.

This article also shares with the research community the Tomato Growth data set [14] collected during the research. The data set contains 5514 time-sequenced top-down images of plant growth and growth conditions. It can be used for training the artificial NNs (ANNs) for solving the problems on plant detection, segmentation, leaf area estimation, and plant growth dynamics assessment.

This article is organized as follows: in Section II, we provide background on the smart agriculture and introduce the reader to the state-of-the-art research in the area. The AI approach is detailed in Section III. Afterward, we present the experimental evaluation with the proposed AI solution for a low-power sensing system in Section IV. Finally, we discuss the obtained results and provide concluding remarks in Section V and Section VI, respectively.

II. Background

Recent success in the smart agriculture domain is mainly powered by the advances in wireless sensor networks (WSNs), 2-D/3-D imaging systems, machine learning, and cloud computing. Although this research and relevant prototypes are still limited, here, we provide concise discussion on the successful attempts in this direction.

The WSN paradigm is a driving force for monitoring and control applications [15] including the control of the climate conditions in a greenhouse [10], [16], [17]. Indeed, environmental monitoring is a reasonably chip solution for greenhouses and tends toward the set-to-forget monitoring option for long periods [18]. Tiny sensors were deployed in difficult-to-access areas at different heights, and measured the greenhouse relative humidity and temperature. This deployment is characterized by the simple control mechanism: the actuators are activated if the threshold values are violated. In this case, the system controls the predefined settings of the greenhouse. Although this study reports on compact wireless sensing devices performing energy-efficient tasks when the measured data are delivered directly to the user or cloud facilities for further processing and/or data storage, it inherently lacks intelligence. It happens due to the limited computation and processing resources on microcontrollers that are not able to run complicated algorithms.

Up to date, AI has been applied for modeling application in agriculture. For example, the machine learning approach is successfully applied for modeling and further estimation of grasslands in Ireland [19]. The authors make the estimation by processing large volumes of available image data. In terms of modeling, three models were developed: ANN, adaptive neuro-fuzzy inference system (ANFIS), and multiple linear regression (MLR).

Imaging approaches include 2-D, 3-D, and, sometimes, 2-D/3-D imaging. The 2-D approach is typically helpful in scenarios when a plant is characterized by a simple structure and rather large leaves as it is analyzed in [20]. At the same time, computer vision and machine learning-based solutions demonstrated their advantages in performing the assessments of fruit characteristics [21]. The disadvantage of 2-D imaging is the complicated software exploited for the image analysis. It suffers from the leaf overlap and concavity. Laser scanning approach is often a good option when a plant digitization is required. It has been successfully applied, for instance, to forestry and canopies statistical analysis [22]. Owing to computationally intensive data processing, its application is limited to the extraction of single-plant attributes.

To overcome the problems that are typical for 2-D imaging, 3-D imaging is used for capturing the shape of the plant and its further analysis in three dimensions. One of these methods is reported in [23]. The authors demonstrate a semiautomatic 3-D imaging system for plant modeling where the reconstructed 3-D points and the actual images are combined. According to this research, more effective segmentation of the data into individual leaves will be guaranteed for the user.

A similar method to our research proposes a 2-D/3-D system enriched with a number of sensors [24], which is able to find the correlations between the leaf area and the biomass. The demonstrated approach assists in predicting the growth rate and the leaf area of the plant. This solution requires a computer or a cloud solution for data processing though.

More detailed reviews of the state-of-the-art smart approaches with a special emphasis on the agriculture domain are present in [1] and [2]. To the best of our knowledge, these works do not report on the deployment of AI on the embedded systems. In addition, they do not target autonomous monitoring, as well as analysis and prediction tasks, in agriculture.

III. AI Approach for Precision Agriculture

A. Problem

Area of the leaves is one of the most important characteristics that represent dynamics and wellness of plant growth. It provides the basics for research in the following areas: plant phenotyping, plant physiology, and plant pathology [25]–[27]. A promising application is the optimization of the plant growth dynamics using the rate of area of the leaves—its changing serves as an indicator of nutrient and energy resource consumption [28], [29]. Area of the leaves can be a good indicator of the total biomass accumulation in the plant, which can be directly used for modeling the plant growth, for the assessment and optimization of the nutrient and energy-resource consumption [30]. For now, it is challenging to develop the automatical, nondestructive, universal, scalable, robust, and precise method for the area of the leaves assessment and prediction. The major bottleneck is high variety of species, huge amount and complexity of underlying processes, and stresses that have an effect on the output, i.e., area of the leaves [31], [32]. There are several types of responses of the plants to the stress: long term and short term. The long-term response typically appears in up to several days. The short-term response to the stress is typically much more damaging and have the time lag of up to 5–6 h [33], [34]. Modeling the plant growth for this period is vital as it allows for predicting and preventing the effects of stress on the plant growth dynamics. It is expected that the accuracy of predictions captures the diurnal fluctuations of the plant growth dynamics (see Section III-C) as it is one of the

main and explicit short-term driving reasons for changing of area of the leaves. Thus, the amplitude of fluctuations can serve as a lowest bound of permissible prediction accuracy. This amplitude varies for different types of nutrient solution (see Section III-C), but in most cases, it has an error in the range of 5%–10% of total area of the leaves.

On the other hand, ubiquitous and efficient application of these models is essential according to the precision agriculture paradigm defined in Section I. For tackling this problem, a low-power sensing solution able to run the models on board and functioning in a distributed manner is required.

B. Method

The design of an industrial plant-growth processes is typically based on the expert knowledge, e.g., of microclimatic requirements, contents of nutrient solution, irrigation schedule, and so on, as well as on the historical experimental data. This approach does not scale and is not generic both in terms of production size and crop variability though.

Recent advances in computational methods, machine learning, and increase in computational power, together with the availability of sensors [35], [36], enabled the collection and processing of enormous amount of data [37]. This progress led to the development of data-driven modeling approaches, e.g., ANNs [38], possessing huge expressive power for high-dimensional data description and generalization.

These methods in conjunction with the surrogate hand-crafted dynamical models [39] are used for recovering the underlying dynamics of complex systems using the collected observations. It is essential to perform the optimization of the control input and achieve the final objective with the lowest expenses, e.g., by picking the best nutrient solution and illumination schedule to lower fertilizer and electricity wasting.

In this article, we use the RNNs for the prediction of the dynamics of plant growth. The RNN is a class of ANNs, where the nodes contain the feedback response and enable the storage of information about their internal state. One of attractive features of the RNNs is that they are potentially able to link previous information with the current state. The RNN can process the data that are represented as time-dependent sequences by using the internal state information. A typical RNN may have a problem with the processing of a long-term dependences. To overcome this problem, the long short-term memory (LSTM) ANNs were introduced as a special architecture of the RNN [13], capable of learning long-term dependences. The key element of LSTM is a cell state, which can be changed in the process of training. This feature is important for modeling the plant growth dynamics, since the future dynamics of the plant growth is in strong relation with the previous states passed long time before.

Recently, many applications for the LSTM NN architecture have appeared [40]. However, for the precision agriculture, the application of the RNN [LSTM or gated recurrent unit (GRU)] for crop yield prediction or description of plant growth dynamics based on the environmental growth conditions is a novel research direction [41]. In this article, we use LSTM as a core of AI and describe it in detail in Section III-C.

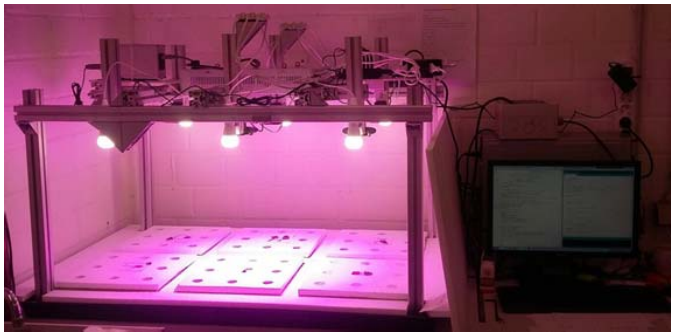

Fig. 1. Experimental setup: growing (bottom) and data collection system (see video cameras on top).

For performing the plant growth modeling and dynamics prediction, we designed an experimental testbed based on the hydroponic approach allowing the simultaneous growth of plants in different conditions (nutrient solutions). This testbed was equipped with an automatic image acquisition system and controlled LED illumination. Then, we conducted one-month experiment on the plant growth and obtained the sequences of raw images of the plant growth with the fixed time interval under different conditions. We developed a software package for calculating the changes in the area of the leaves in time based on the obtained images. Using this algorithm, the area of the leaves was calculated during the experiment. The data on area of the leaves were used for training the NNs and other machine learning algorithms.

Afterward, we performed the ablation study and tried out several machine learning algorithms, NNs architectures, and types of neurons to identify the optimal solution for our problem, i.e., the precise prediction dynamics of plant growth. The best RNN LSTM architecture was trained using the optimal learning parameters. In addition, an important requirement for the proposed RNN is a small amount of trainable parameters, since it is crucial for its running on a low-power sensing system.

C. Verification

1) Experimental Setup and Measuring System: The experimental setup based on the hydroponic approach to grow the plants and coupled with an imaging system was designed and assembled for obtaining image and condition data describing the plant growth (see Fig. 1). This system makes it possible to grow up to 54 small plants, e.g., dwarf tomatoes, to monitor their growth by cameras concurrently and automatically. In our experiment, we grew 48 dwarf tomatoes MicroTina [42]. We separated a tray for growing plants into six isolated sections. In each of them, the plants were fed using different feeding solutions. Each of the sections contained eight plants. They were fed manually and were grown in a 0.65-L rock wool block. The tray was covered by the foam plastic to facilitate the postprocess of images. The imaging system contained six high-resolution cameras Logitech c920 mounted above each section on a regulated platform. The artificial illumination of the plants was provided with a 150-W Neususs LED. Additional white LED illumination was added and switched on while the

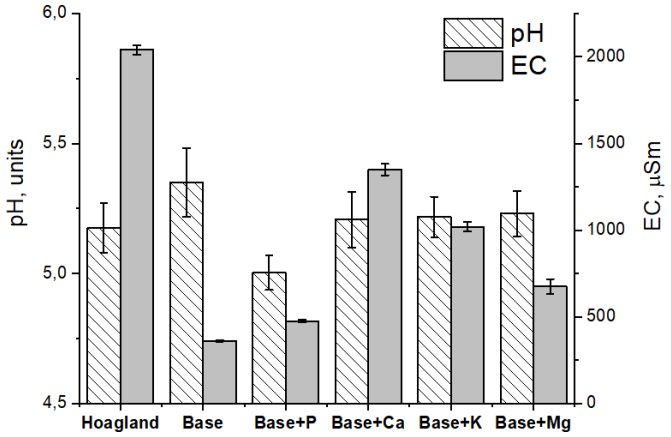

Fig. 2. Properties of the nutrient solutions: pH and EC. Properties were measured for each type of nutrient solutions that were prepared four times during the experiment.

cameras took photos. The automatically controlled day/night light duty cycle made 17/7 h. It was slightly decreased by the end of the experiment to 15/9 h due to plant physiology reasons.

In the beginning of the experiment, 70 seeds of MicroTina [42] were germinated in a small rock wool cartridge in a separate tray under LED light with a 17-h duty cycle (from 1 A.M. to 6 P.M.) at a 0.6-m distance. The commercial nutrient solution in the amount of 1.3 L was used for the germination of all seeds (Vostex concentration: 0.5 mL/L of water). A special type of solution for each section was prepared. There were five feeding solutions that contained the base feeding solution, which is the output of the filtering system. To this "Base" solution, special additives (P, K, Ca, Mg, and microelements) were added. The other one is the reference solution known as the "Hoagland" nutrient solution [43]. Then, 48 of 70 seeds that had already been propagated were put into the experimental setup. Each rock wool block from a particular section was watered with 0.5 L of a solution prepared for a section, respectively (for eight blocks, 4 L of each solution was initially used). The experiment was conducted slightly longer than one month; the solutions, therefore, were prepared four times. Properties, such as pH and electrical conductivity (EC) of the prepared nutrient solutions, are presented in Fig. 2. EC and pH were measured with ± 0.5 μSm and ± 0.005 accuracy, respectively. It is essential to prepare solutions with the same EC for ensuring similar conditions in each section of the plant growth. Deviation in the pH level is not crucial, since, for each type of the solution, it should be in certain range. Every day at around 15:00, each plant was fed with 20 mL of nutrient solution.

2) Image Data Acquisition and Elaboration: During this experiment, images of each section with plants were automatically taken and recorded every 30 min. In total, we obtained 5514 raw images having a strict time dependence. Examples of raw images are shown in Fig. 3. These images were used for the automatic calculation of the leaf area. The data obtained were used to train the NN to predict the area of the leaves. The leaf area calculation algorithm was based on the algorithm described in the article [44]. The general idea of the algorithm

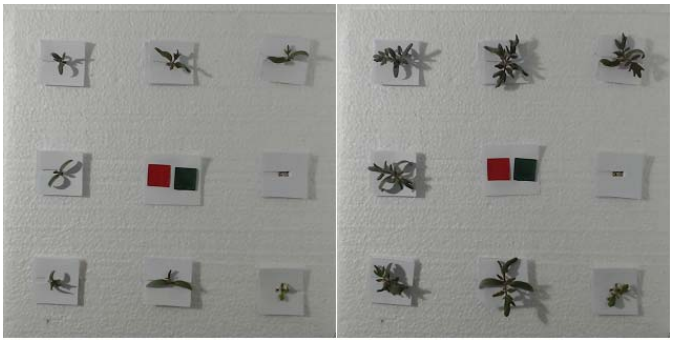

Fig. 3. Example of top-down photographs obtained in the experiment. Left: tomatoes on the fifth day after germination. Right: tomatoes on the tenth day after germination.

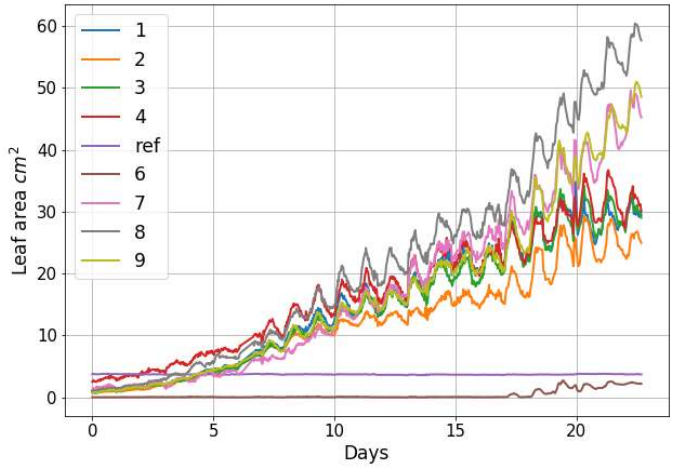

(a)

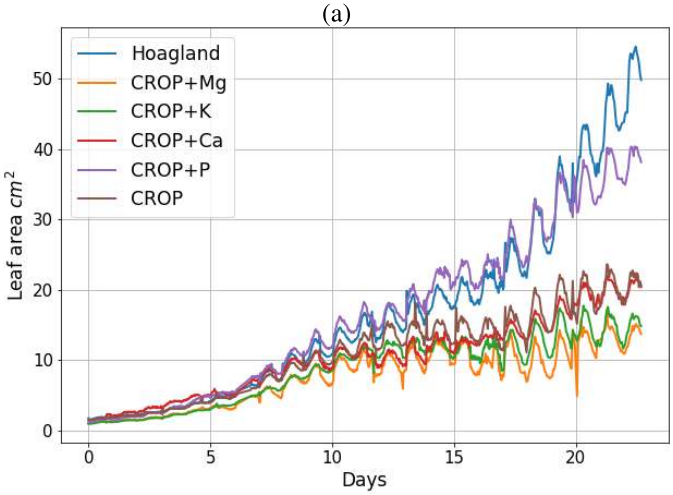

(b)

Fig. 4. (a) Example of area of the leaves calculation for dwarf tomato plants that were grown in section with "Base + P" feeding. (b) Average area of the leaves of plants in each growing section with the corresponding feeding solution.

is to calculate the "green" pixels in the image. Bounds in RGB pallet were adapted in the code to recognize "green" pixels for the exact sort of plant and illumination. Using the reference object with the known area, the leaf area was reconstructed in the real-world units.

Prior to starting the experiment, we calibrated the camera and the algorithm for leaf area calculation. We took the same sort of tomato that was used in the experiment, cut out the

part of the leaf of a certain area (we tried 0.5, 1, and 2 cm^2 leaf areas), recalculated the leaf area relative to the label with a known area (red square with a known area), and set up the algorithm and lighting, trying to minimize the error in determining the area of the leaves. We also performed a similar calibration procedure for different parts of the camera field of view. During the main experiment, the same illumination as in the calibration procedure was used. The leaf area of the tomatoes was not measured directly during the experiment, but several control point checks of the algorithm and the camera were carried out. Due to the fact that during these checks it is necessary to stop the experiment for about 5 min, we tried to avoid these checks frequently though. During checking, we added a part of leaf with manually measured area in the camera field of view. We estimated the reference leaf area by taking two consecutive pictures of only tomatoes and tomatoes with the reference. Then, the leaf area obtained from one picture with the reference was subtracted from a leaf area obtained from another picture without the reference. As a result of these checks at various stages of the experiment, no serious deviations in the operation of the system and an estimate of the surface area of the foliage were found.

Fig. 4(a) shows an example of the leaf area calculations for each tomato plant fed by the nutrient solution "Base + P." We also calculated the average area of the leaves for each section (each feeding solution). Fig. 4(b) shows the average area of the leaves for plant in each section, from which we can conclude which additive to the base solution is best. In our case, phosphorus additives have the best effect among others. It is highly important that we can numerically estimate the effect of different factors on plant growth dynamics by using simple cameras. This opens a wide possibility to drive plant growth process in the most useful direction. Totally, we obtained 44 112 measurements of the leaf area projection. It should be noted that the estimation of the leaf area was done by measuring its maximum projection, which, in general, may not be equal to the real leaf area. However, these measurements also can give us additional information about the hidden dynamics of the plant growth. For example, we can observe diurnal fluctuations in the relative leaves positions in Fig. 4(a) caused by biological processes. This additional information can be included into the predictive model making it more precise. As we do not use the classical statistical methods, we can directly use our data as an input to our NN without error estimation.

3) Performance Evaluation: We conducted calculation experiments by using the data for 12 days and trained the LSTM model for each section. The data set was split into the training and test sets with 400 and 200 elements for each section, respectively.

We used the Adam optimizer [45] and the mean squared error as a loss function. For the Adam optimizer, we used hyperparameters: lr $= 0.001$ (learning rate); $\text{beta}_1 = 0.9$ (exponential decay rate for the first moment); $\text{beta}_2 = 0.999$ (exponential decay rate for the second moment); epsilon $= 10^{-8}$. We reset the hidden states for each epoch of training. The network was trained for ten epochs, which is a reasonable amount for the stabilization of the loss function for

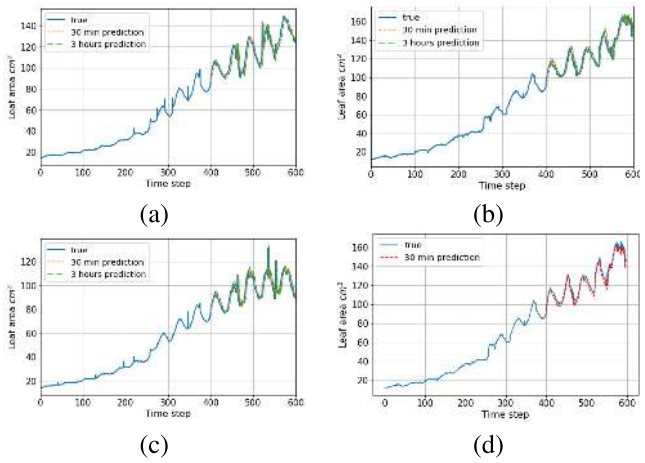

Fig. 5. (a) Prediction of a leaf area for section that fed with "Hoagland" nutrient solution. (b) Prediction of a leaf area for section that fed with "Base + P" nutrient solution. (c) Prediction of a leaf area for section that fed with "Base + Ca" nutrient solution. (d) Prediction of a leaf area based on autoregression for section that fed with "Base + P" nutrient solution. Each time step in (a), (b), and (d) represents 30 min.

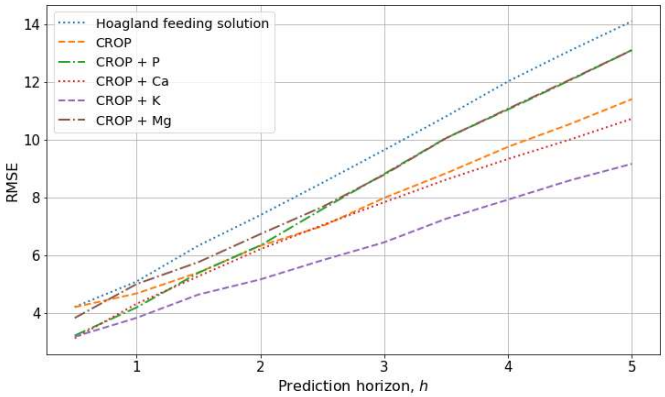

Fig. 6. Dependence of root mean square errors for the prediction of leaf area on the number of prediction steps for all six solutions.

the most of the tested architectures with one hidden layer of LSTM. We tried different amount of points from the previous steps for doing predictions and realized that a three-point set is enough for doing accurate predictions even for 3-h horizon. The train/test data set was created in the following way. Each train/test data sample contained 13 points: sequence of three points (leaf area) from the previous three steps and sequence of ten points for the next ten steps. Data set preparation process also included transformation to stationary time series and scaling to $(-1{:}1)$ range. In this article, we evaluate the root mean square error (RMSE) of predictions for time horizon from 30 min to 5 h.

The results of leaf area (projection) prediction presented for three out of six possible options (six different solutions were in the experiment) are shown in Fig. 5(a)–(c). The leaf area in Fig. 5(a)–(c) was taken as a sum of area of the leaves of all the plants in the section. Diurnal fluctuations were also predicted by our trained model. This result allows us to assess real area of the leaves by the interpolation of the resulting curve on top. The results of this prediction demonstrate good fit to the ground truth. RMSE in Fig. 6

TABLE I
PERFORMANCE OF DIFFERENT ARCHITECTURES OF LSTM NNs

Amount of LSTM neurons	RMSE for 0.5/3 h prediction horizon	Amount of trainable p-rs
2	3.25/9.01	62
10	3.19/8.72	670
2/2	3.27/9.2	118
2/4	3.2/8.9	210
4	3.18/8.6	178

shows how the error changes with respect to the size of step prediction. It is worth noting that we have good prediction even for the 5-h prediction horizon. Since RMSE varies from 9 to 14 for different solutions for a 5-h prediction horizon and from approximately 100 to 140 for the test data set area of the leaves values, we demonstrated that the obtained performance withstands the application requirements even for the 5-h horizon (maximum that is required): 5%–10% of relative error. For the lower prediction horizon, the relative error is less. We note here that this experiment was conducted in the closed artificial system.

4) Comparative Study on RNN Architectures and Methods: We also performed the ablation study where we tested different amount of neurons and different architectures. Some of the results that are calculated for the section with "Base + P" feeding solution are presented in Table I. As an example, for two LSTM units, there are 62 trainable parameters and the RMSE is 3.25 and 9.01 for the 30-min and 3-h prediction horizon, respectively. For ten LSTM units, there are 670 trainable parameters (which is not acceptable as we have 400 data samples for training and the common rule is that the amount of estimated parameters should be less than the train set size) and the RMSE is 3.19 and 8.72 for the 30-min and 3-h prediction horizon, respectively. If we use two-layer LSTM NN, then, in the case of two LSTM units on each layer, we get RMSE 3.27 and 9.2 for the 30-min and 3-h prediction horizon, respectively, and in the case of four LSTM units on each layer, we get RMSE 3.2 and 9.0 for the 30-min and 3-h prediction horizon, respectively. Based on these findings, we decided to use LSTM with four units as a compromise between the amount of parameters (178), accuracy (RMSE is 3.18 and 8.6 for the 30-min and 3-h prediction horizon, respectively), and complexity.

We also compared the performance of LSTM with the performance of four units GRU RNN with 146 parameters. The RMSE is 3.21 and 8.7 for the 30-min and 3-h prediction horizon, respectively, for GRU-RNN. It means that it is also possible to use other highly efficient types of RNNs for our purposes. The same amount of epochs, i.e., 10, was used for training the RNN with GRU neurons. The Adam optimizer with the same parameters as for the LSTM RNN was used. Moreover, implemented for the GRU-RNN, the data preparation procedure including the transformation to the stationary time series, scaling, and splitting to the train/test data set was equal to the tested LSTM RNN. For the other nonrecurrent approaches, e.g., convolutional neural network (CNN) over a window data, 50 epochs are needed for convergence reasons. Nonrecurrent approaches were also tested. Prediction is based on the CNN over a window of data. We used 1-D convolution with 16 filters and kernel size $=$ 2. Then, we used max pooling and dense layers with ReLU activation. The data prepossessing procedure was the same as for the LSTM RNN; however, 50 epochs are required for convergence and loss stabilization. The amount of parameters is 328 and accuracy (RMSE) is 3.71 and 9.7 for the 30-min and 3-h prediction horizon, respectively. This result is worse than the LSTM architecture used in this article and more parameters have to be estimated. Increasing the amount of filters/layers leads to dramatic increase in the amount of training parameters, while a small number of training parameters are crucial for our data set. In fact, the best result was achieved while using simple methods based on autoregression [see Fig. 5(d)]. For window size 10, RMSE $=$ 4.61 (excellent result over all window sizes and approximately 40% worse than for LSTM), for window size 2, RMSE reached 7.91. Based on this research, we realized that LSTM showed its robustness compared with simpler approaches. We investigated how newly obtained data during the experiment could improve the accuracy and whether it is important to retrain our system. For doing this, we conducted tests with several splitting options of the data set. Four-hundred data samples in the training set showed the acceptable accuracy of the predictions and further increase of training samples does not significantly improve the accuracy. It means that we do not need to retrain the NN during this time period for achieving more precise results, and this is highly important, since the embedded sensing system with AI on board works only with the pretrained NNs—there is no need to upload newly trained NN periodically, which leads to the decrease in system autonomy.

IV. LOW-POWER SENSING SYSTEM WITH AI: EXPERIMENTAL EVALUATION

A. System Overview

The LSTM NN architecture described in Section III-C was implemented, trained, and tested on a desktop computer. However, the real challenge for the NNs is their implementation and running on the low-power embedded and mobile systems that are not initially designed for data-intensive computing.

In our experimental study, the ultimate goal is to demonstrate the feasibility of the proposed approach in Section III and the opportunity to implement the predictive analytics on board of a low-power embedded system. It helps solving real-world problems in the scope of precision agriculture and, in particular, modeling of the plant growth dynamics.

Since the idea behind the precision agriculture is to ensure intelligent, distributed, and autonomous sensing, we define the following requirements for a tiny sensor node.

1) *Size [mm]:* $100 \times 60 \times 20$.
2) Mass $<$ 100 [g].
3) *Processor Performance:* Quad-core 0.9 [GHz].
4) RAM $>$ 300 [Mb].
5) Power consumption (Idle) $<$ 5 [W].
6) *OS:* Linux.
7) *Interface:* USB 2.0 or later.
8) *Wireless Connectivity:* Wi-Fi.
9) Price $<$ 100$.

TABLE II
SINGLE-BOARD COMPUTER TRADEOFF STUDY

SBC	Mass	Processor	RAM	Power
Raspberry Zero	9.0 g	1 GHz	512 Mb	5 W
Raspberry Pi 3B	45 g	1.2 GHz	1 Gb	1.6 W
ODROID - C2	56 g	1.5 GHz	2 Gb	5 W
UP Board	56 g	1.44 GHz	4 Gb	3.4 W
Orange Pi PC	32 g	1.53 GHz	1 Gb	1.02 W
Banana Pi	48 g	1 GHz	1 Gb	1.6 W
ASUS Tinker Board	55 g	1.8 GHz	2 Gb	2.25 W

The size, mass, and power consumption are important parameters for the system deployment in a greenhouse or climate chamber. Processor and RAM requirements are essential for running the AI discussed earlier. The USB interface is required for plugging a camera or connecting external devices, e.g., sensors. The last requirement is about the wireless connectivity: Wi-Fi is a widely used technology in distributed wireless sensing for connecting the sensor nodes to a network. Wireless network evaluation is out of the scope of this article—we demonstrate the operation of a single node, which is a consistent part of the future system.

For choosing a proper embedded system able to run an AI algorithm on board, we conduct a comparative study on the popular systems available on the market. Obviously, the list shown in Table II could be significantly extended as the mentioned requirements could be met by many state-of-the-art platforms. That is why we introduced extra requirements, e.g., "Size," Operating System "OS," and "Price," which on the one hand are relevant for ensuring stable operation and ubiquitous deployment and, on the other hand, help cut off the list of platforms.

For our experimental study, we chose Raspberry Pi 3B, which meets most requirements and can be further optimized in terms of power consumption and performance. It is worth noting that we use an external neural computer stick (NCS) Movidius connected to the embedded system by a USB interface and able to run the NNs.

B. Hardware

The prototype is implemented using Raspberry Pi with the external graphics processing unit (GPU) Intel Movidius based on the *Myriad* processor [46]. It is a low-power external processor for running the pretrained NNs on the computing systems with restricted computational capabilities. The processor has 12 programmable vector engines and has computational performance around 100 GFLOPS at 1-W power consumption. Its capability allows for simultaneous processing of data from eight HD sensors. It has up to 450-Gb/s carrying capacity. The prototype also has the 5-in HDMI display for the interaction with the user. The system is powered by a 2550-mAh battery. This capacity is enough to guarantee the autonomous operation of the system for two months—the growth cycle of the tomatoes. The block diagram of the prototype is shown in Fig. 7.

The major disadvantage of the embedded system with the AI is that the training of NNs is impossible. Even though it can work only with the pretrained networks, these can

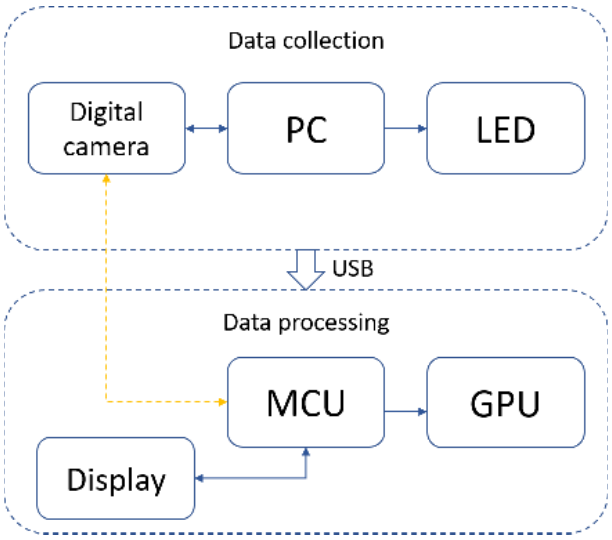

Fig. 7. Block diagram of the proposed intelligent low-power sensing system for precision agriculture.

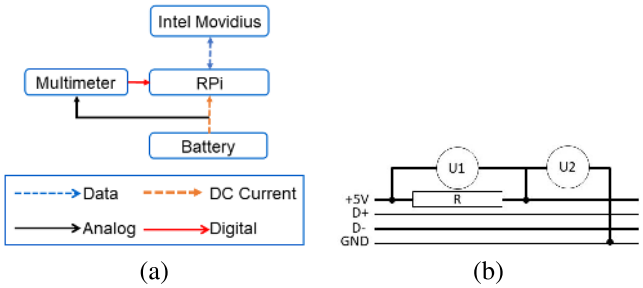

Fig. 8. (a) Block diagram of the experimental testbed. (b) Connection of the multimeter probes to the Raspberry Pi power rode.

be the sophisticated architectures of CNNs as well as deep NNs (DNNs). The LSTM model was implemented on the prototype in the following way: the model was trained on a desktop using Python 3 with Keras library. Then, the Keras model was converted into the TensorFlow model and compiled to the binary graph by means of the Movidius Neural Compute (MVNC) library provided by Intel. We used Keras library version 2.1.6 for creating and training NNs with TensorFlow library version 1.2.1 for backend calculations.

C. System Assessment

1) Experimental Setup and Measuring System: Experimental testbed is shown in Fig. 8(a). All the calculations are run on Raspberry Pi: it receives and processes the data, then sends the data to the external GPU (Intel Movidius), and receives back the prediction. This process goes simultaneously with the collection of the power consumption data. For this reason, we designed a custom multimeter based on the ATmega328P 8-bit microcontroller. It features a 10-bit successive approximation analog-to-digital converter (ADC). The accuracy of the ADC is $+/-$ twice the value of the least significant bit.

We designed a custom-made multimeter, since the data on the power consumption and computational performance are received simultaneously during the tests carried out on the

TABLE III
COMPARATIVE STUDY OF COMPUTER AND EMBEDDED INTELLIGENCE (PROTOTYPE)

Characteristics	Computer: ASUS UX305CA	Prototype: Raspberry Pi 3B with Intel Movidius
Processor	Quad-core 64 bit Intel(R) Core() m3-6Y30 (0.9 - 1.51 GHz)	Quad-core 64-bit ARM Cortex A53 (1.2 GHz)
RAM	4 Gb (shared with GPU)	1 Gb (shared with GPU)
GPU	Intel(R) HD Graphics 515 @300 MHz base @850 MHz maximum	Broadcom VideoCore IV @ 400 MHz and external GPU - Intel Movidius (Myriad 2)
Power Storage Capacity	Li-ion 45 Wh	Li-ion 18.87 Wh
Power Consumption in Idle mode	4.5 W	1.5 W (Raspberry Pi) + 1 W (Movidius)
Max time of operation	10 hours	7.5 hours

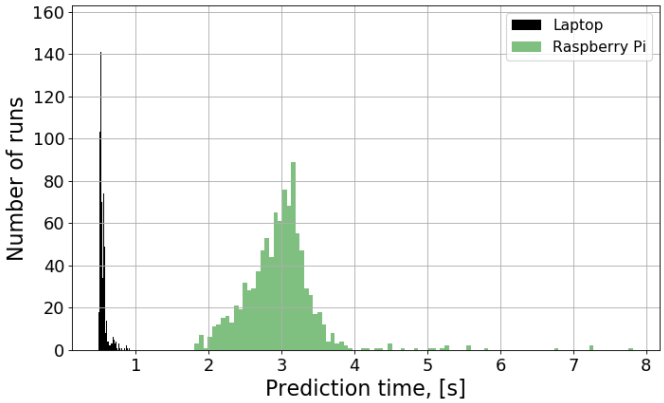

Fig. 9. Histogram of run-time distribution. Green bars: Raspberry Pi. Gray bars: computer.

board of RPi. That is why we need to process it synchronously. The multimeter is calibrated using the APPA 505 laboratory multimeter. In terms of measurement methodology, we relied on the research reported in [47].

We connect the multimeter to the power rode of the Raspberry Pi by the 100-mΩ 1% shunt [see Fig. 8(b)], which receives the volt–ampere (VA) characteristics and sends the digital data to the COM-port of RPi. We get the computational and power consumption-related characteristics and record them into ".csv" table. These characteristics include timestamp, test and train scores, VA, power consumption, CPU, and RAM usage.

The experiment includes the following steps.

1) Analysis of the overall computational performance of the system.
2) Time estimation of the code execution for a single prediction step.
3) Measurement of power consumption.

Power consumption is calculated as follows:

$$P = U_2 * U_1 / R \tag{1}$$

where U_2 is the voltage, measured on the power rode, U_1 is the voltage on the shunt, and R is the shunt resistance.

2) Results: This experiment is performed for the proposed low-power embedded system and for a desktop that are characterized by the parameters summarized in Table III.

Pretrained LSTM was uploaded to both the platforms with the test data set. After that, the NN iteratively performed the predictions. The total number of iterations is 1000. In every single run, the model and the test data set were refreshed. During the investigation, the root mean square error and the time spent for a single prediction were measured (see Fig. 9). The "prediction time" was measured as the difference between the final and the start time of a single run of the prediction algorithm. Fig. 9 shows that the time per prediction varies over the experiment for both platforms especially for the RPi with NCS. It is featured with lower computational performance and, hence, the increased possibility of buffer overflow.

TABLE IV
PERFORMANCE EVALUATION OF COMPUTER AND EMBEDDED INTELLIGENCE PROTOTYPE

Parameter	Computer	Prototype
Median prediction time, s	0.55	2.98
Maximum prediction time, s	1.26	7.82
Minimum prediction time, s	0.49	1.81

The computational performance of the computer as compared with the Raspberry Pi is roughly six times higher as it is shown in Table IV.

RMSE for the experimental testbed remains constant for every iteration for both Raspberry Pi and computer and equals to 8.30. Each prediction is made by the NN, trained on a data set with 400 elements (one element is the one-time step, which equals to 30 min) and every prediction is made for the following 200 steps. The operation period of the system is 30 min. During that period, the system starts, gets picture, processes it, and feeds the data to the NN. It takes around 30 s. It is in sleep mode for the rest of the time; hence, the duty cycle is 3.4%. Mean time for booting up is around 20 s; it takes 7 s to get and process the picture; and prediction time varies from 1.8 to 7.8 s with a median value of 3 s.

The computational performance is low mostly due to the absence of USB 3.0 interface on the board of Raspberry Pi 3B, whereas Movidius is equipped with it. Even though the single-board computer with Movidius has higher prediction time, it is still much faster than needed. For the current problem, each prediction should be performed every 30 min or more frequently.

For assessing the long-term operation of the proposed embedded AI system, we used a 2550-mAh power bank and run the sequence "load model—load test set—make prediction" in a loop. In this experiment, we measured the power consumption over the iterations (see Fig. 10).

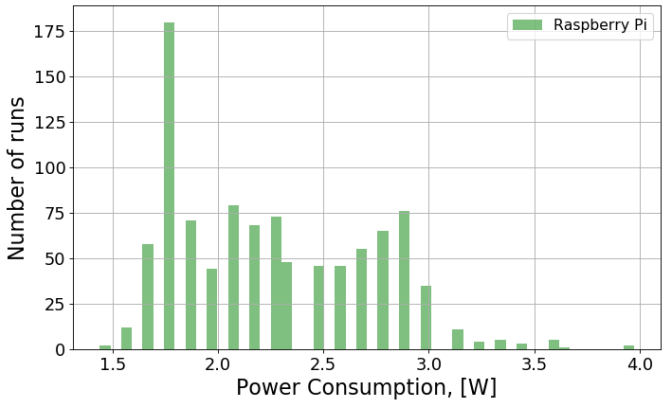

Fig. 10. Power consumption of the prototype over runs.

V. Discussion

In this article, we designed a testbed for data collection in the lab environment (see Fig. 1) and an intelligent low-power sensing prototype for deployment in a real greenhouse. The testbed has the LED-based susbsystem for ensuring the illumination, while the prototype requires an external source of light. The proposed prototype is a scalable solution, which is easy to deploy as a distributed system in the greenhouses without an additional hardware and infrastructure.

According to our investigation, the prototype can perform 8663 continuous predictions within 4 h 34 min before the battery discharge. The mean prediction time is 1.9 s. The mean power consumption during the investigation is 2.23 W, median is 2.184 W, and modal value of power consumption is 1.7578 W. The CPU load during the experiment was 52.44% with standard deviation 3.22 and 50.8% of RAM with standard deviation 0.19. Because of the continuous and slow change of the plants state, there is no need to perform these predictions continuously: the 3-h time step is sufficient and still provides high precision of predictions. Since the system is assumed to switch ON and OFF every 30 min and perform one prediction within this time period, the system can operate autonomously for up to 180 days until the battery is completely depleted. The obtained performance withstands the application requirements discussed in Section IV-B.

That is why the proposed solution proves to be an efficient low-power system with AI on board. It can be beneficial to the applications where the low power consumption, low mass and size, and autonomous operation are required. The system can be easily extended and adopted to the mobile platforms, e.g., drones. In this case, a digital camera can be added to it along with the embedded leaf-area-calculating algorithm. If realized into practice, this system will close the gap and will be able to perform the full cycle of plant growth dynamic analysis.

Power consumption of the platform varies within the time of experiment. This value correlates with the time period spent for the prediction task. Since it is a pilot study, there will be many unpredicted factors in a real deployment influencing the performance, e.g., reducing the system performance and increasing the power consumption (see Figs. 9 and 10). We assume that the primary factor having the influence on the system performance is the limited RAM and cache memory of Raspberry Pi. It leads to the memory overflow that has a negative impact on the power consumption.

VI. Conclusion

In this article, we have presented a generic low-power embedded platform equipped with the AI on board for assessing and predicting the plant growth dynamics.

Performance evaluation of the proposed solution has demonstrated that the developed AI architecture based on an RNN called the LSTM is characterized by reasonable precision for horizon of prediction. The proposed solution can be used as an autonomous tool for the continuous plant growth dynamics monitoring for up to 180 days. Together with an actuating capability, the proposed approach is promising for guaranteeing an easy-to-deploy, generic, and robust optimization tool for the precision agriculture.

The Tomato Growth data set [14] for the training and testing procedures was collected by the designed and assembled experimental setup coupled with the automatic imaging system. This data set is publicly available for research community. It can be used in a variety of computer vision tasks for the development and verification of new machine learning algorithms. For effectuating the growing stage on the experimental setup, we used a hydroponic approach. It ensures the optimal control of the plant nutrition and provides the opportunity to "drive" the system in a desirable way.

References

[1] O. Elijah, T. A. Rahman, I. Orikumhi, C. Y. Leow, and M. N. Hindia, "An overview of Internet of Things (IOT) and data analytics in agriculture: Benefits and challenges," *IEEE Internet Things J.*, vol. 5, no. 5, pp. 3758–3773, Oct. 2018.

[2] K. Taylor *et al.*, "Farming the Web of Things," *IEEE Intell. Syst.*, vol. 28, no. 6, pp. 12–19, Nov./Dec. 2013.

[3] L. Zhou, N. Chen, Z. Chen, and C. Xing, "Roscc: An efficient remote sensing observation-sharing method based on cloud computing for soil moisture mapping in precision agriculture," *IEEE J. Sel. Topics Appl. Earth Observ. Remote Sens.*, vol. 9, no. 12, pp. 5588–5598, Dec. 2016.

[4] N. D. Lane, S. Bhattacharya, A. Mathur, P. Georgiev, C. Forlivesi, and F. Kawsar, "Squeezing deep learning into mobile and embedded devices," *IEEE Pervasive Comput.*, vol. 16, no. 3, pp. 82–88, Jul. 2017.

[5] A. Chaudhury *et al.*, "Computer vision based autonomous robotic system for 3d plant growth measurement," in *Proc. 12th Conf. Comput. Robot Vis. (CRV)*, Jun. 2015, pp. 290–296.

[6] P. Eugster, V. Sundaram, and X. Zhang, "Debugging the Internet of Things: The case of wireless sensor networks," *IEEE Softw.*, vol. 32, no. 1, pp. 38–49, Jan./Feb. 2015.

[7] A. H. Alavi, P. Jiao, W. G. Buttlar, and N. Lajnef, "Internet of Things-enabled smart cities: State-of-the-art and future trends," *Measurement*, vol. 129, pp. 589–606, Dec. 2018.

[8] P. C. P. De Silva and P. C. A. De Silva, "Ipanera: An industry 4.0 based architecture for distributed soil-less food production systems," in *Proc. Manuf. Ind. Eng. Symp. (MIES)*, Oct. 2016, pp. 1–5.

[9] L. Li, Q. Zhang, and D. Huang, "A review of imaging techniques for plant phenotyping," *Sensors*, vol. 14, no. 11, pp. 20078–20111, Oct. 2014.

[10] R. Pahuja, H. K. Verma, and M. Uddin, "A wireless sensor network for greenhouse climate control," *IEEE Pervasive Comput.*, vol. 12, no. 2, pp. 49–58, Apr./Jun. 2013.

[11] F. Rodríguez, M. Berenguel, J. L. Guzmán, and A. Ramírez-Arias, *Modeling and Control of Greenhouse Crop Growth*. Springer, 2015.

[12] H. Vereecken *et al.*, "Modeling soil processes: Review, key challenges, and new perspectives," *Vadose Zone J.*, vol. 15, no. 5, pp. 1–57, May 2016.

[13] S. Hochreiter and J. Schmidhuber, "Long short-term memory," *Neural Comput.*, vol. 9, no. 8, pp. 1735–1780, 1997.

[14] D. Shadrin, A. Menshchikov, A. Somov, G. Bornemann, J. Hauslage, and M. Fedorov. (2019). *Tomato Growth Dataset*. Accessed: Jan. 21, 2019. [Online]. Available: https://github.com/DmitriiShadrin/TomatoesGrowth

[15] A. Somov, A. Baranov, D. Spirjakin, A. Spirjakin, V. Sleptsov, and R. Passerone, "Deployment and evaluation of a wireless sensor network for methane leak detection," *Sens. Actuators A, Phys.*, vol. 202, pp. 217–225, Nov. 2013.

[16] O. Mirabella and M. Brischetto, "A hybrid wired/wireless networking infrastructure for greenhouse management," *IEEE Trans. Instrum. Meas.*, vol. 60, no. 2, pp. 398–407, Feb. 2011.

[17] G. R. Mendez, M. A. M. Yunus, and S. C. Mukhopadhyay, "A WiFi based smart wireless sensor network for monitoring an agricultural environment," in *Proc. IEEE Int. Instrum. Meas. Technol. Conf.*, May 2012, pp. 2640–2645.

[18] L. Lombardo, S. Corbellini, M. Parvis, A. Elsayed, E. Angelini, and S. Grassini, "Wireless sensor network for distributed environmental monitoring," *IEEE Trans. Instrum. Meas.*, vol. 67, no. 5, pp. 1214–1222, May 2018.

[19] I. Ali, F. Cawkwell, E. Dwyer, and S. Green, "Modeling managed grassland biomass estimation by using multitemporal remote sensing data—A machine learning approach," *IEEE J. Sel. Topics Appl. Earth Observ. Remote Sens.*, vol. 10, no. 7, pp. 3254–3264, Jul. 2017.

[20] K. Rajendran, M. Tester, and S. J. Roy, "Quantifying the three main components of salinity tolerance in cereals," *Plant, Cell Environ.*, vol. 32, no. 3, pp. 237–249, Mar. 2009.

[21] P. Pouladzadeh, S. Shirmohammadi, and R. Al-Maghrabi, "Measuring calorie and nutrition from food image," *IEEE Trans. Instrum. Meas.*, vol. 63, no. 8, pp. 1947–1956, Aug. 2014.

[22] X. Yang *et al.*, "Three-dimensional forest reconstruction and structural parameter retrievals using a terrestrial full-waveform lidar instrument (Echidna)," *Remote Sens. Environ.*, vol. 135, pp. 36–51, Aug. 2013.

[23] L. Quan, P. Tan, G. Zeng, L. Yuan, J. Wang, and S. B. Kang, "Image-based plant modeling," *ACM Trans. Graph.*, vol. 25, no. 3, pp. 599–604, 2006.

[24] D. Shadrin, A. Somov, T. Podladchikova, and R. Gerzer, "Pervasive agriculture: Measuring and predicting plant growth using statistics and 2D/3D imaging," in *Proc. IEEE Int. Instrum. Meas. Technol. Conf. (IMTC)*, May 2018, pp. 1–6.

[25] H. Scharr *et al.*, "Leaf segmentation in plant phenotyping: A collation study," *Mach. Vis. Appl.*, vol. 27, no. 4, pp. 585–606, 2016.

[26] N. An *et al.*, "Plant high-throughput phenotyping using photogrammetry and imaging techniques to measure leaf length and rosette area," *Comput. Electron. Agricult.*, vol. 127, pp. 376–394, Sep. 2016.

[27] G. T. Freschet, E. M. Swart, and J. H. Cornelissen, "Integrated plant phenotypic responses to contrasting above- and below-ground resources: Key roles of specific leaf area and root mass fraction," *New Phytologist*, vol. 206, no. 4, pp. 1247–1260, Jun. 2015.

[28] H. Medrano *et al.*, "From leaf to whole-plant water use efficiency (WUE) in complex canopies: Limitations of leaf wue as a selection target," *Crop J.*, vol. 3, no. 3, pp. 220–228, Jun. 2015.

[29] M. Kang and F.-Y. Wang, "From parallel plants to smart plants: Intelligent control and management for plant growth," *IEEE/CAA J. Automatica Sinica*, vol. 4, no. 2, pp. 161–166, Apr. 2017.

[30] S. M. Weraduwage, J. Chen, F. C. Anozie, A. Morales, S. E. Weise, and T. D. Sharkey, "The relationship between leaf area growth and biomass accumulation in arabidopsis thaliana," *Frontiers plant Sci.*, vol. 6, p. 167, Apr. 2015.

[31] A. Singh, B. Ganapathysubramanian, A. K. Singh, and S. Sarkar, "Machine learning for high-throughput stress phenotyping in plants," *Trends Plant Sci.*, vol. 21, no. 2, pp. 110–124, Feb. 2016.

[32] Z. C. Campbell, L. M. Acosta-Gamboa, N. Nepal, and A. Lorence, "Engineering plants for tomorrow: How high-throughput phenotyping is contributing to the development of better crops," *Phytochem. Rev.*, vol. 17, no. 6, pp. 1329–1343, Dec. 2018.

[33] J. Roy, *Response of Plants to Multiple Stresses*. New York, NY, USA: Academic, 2012.

[34] E. Acevedo, T. C. Hsiao, and D. Henderson, "Immediate and subsequent growth responses of maize leaves to changes in water status," *Plant Physiol.*, vol. 48, no. 5, pp. 631–636, Nov. 1971.

[35] G. Mois, S. Folea, and T. Sanislav, "Analysis of three IoT-based wireless sensors for environmental monitoring," *IEEE Trans. Instrum. Meas.*, vol. 66, no. 8, pp. 2056–2064, Aug. 2017.

[36] J. Gutiérrez, J. F. Villa-Medina, A. Nieto-Garibay, and M. Á. Porta-Gándara, "Automated irrigation system using a wireless sensor network and GPRS module," *IEEE Trans. Instrum. Meas.*, vol. 63, no. 1, pp. 166–176, Jan. 2014.

[37] N. Davies and S. Clinch, "Pervasive data science," *IEEE Pervasive Comput.*, vol. 16, no. 3, pp. 50–58, Jul. 2017.

[38] S. Piersanti and A. Orlandi, "Genetic algorithm optimization for the total radiated power of a meandered line by using an artificial neural network," *IEEE Trans. Electromagn. Compat.*, vol. 60, no. 4, pp. 1014–1017, Aug. 2018.

[39] D. Shadrin, A. Chashchin, G. Ovchinnikov, and A. Somov, "System identification—Soilless growth of tomatoes," in *Proc. IEEE Int. Instrum. Meas. Technol. Conf. (IMTC)*, May 2019, pp. 602–607.

[40] M. F. Stollenga, W. Byeon, M. Liwicki, and J. Schmidhuber, "Parallel multi-dimensional LSTM, with application to fast biomedical volumetric image segmentation," in *Proc. Adv. Neural Inf. Process. Syst.*, 2015, pp. 2998–3006.

[41] A. Chlingaryan, S. Sukkarieh, and B. Whelan, "Machine learning approaches for crop yield prediction and nitrogen status estimation in precision agriculture: A review," *Comput. Electron. Agricult.*, vol. 151, pp. 61–69, Aug. 2018.

[42] J. Scott, B. Harbaugh, and E. Baldwin, "'Micro-tina' and 'micro-gemma' miniature dwarf tomatoes," *HortScience*, vol. 35, no. 4, pp. 774–775, Jul. 2000.

[43] D. R. Hoagland *et al.*, "The water-culture method for growing plants without soil," *Circular. California Agricult. Exp. Station*, vol. 347, no. 2, pp. 1–31, 1950.

[44] H. M. Easlon and A. J. Bloom, "Easy leaf area: Automated digital image analysis for rapid and accurate measurement of leaf area," *Appl. Plant Sci.*, vol. 2, no. 7, May 2014, Art. no. 1400033.

[45] D. P. Kingma and J. Ba, "Adam: A method for stochastic optimization," Dec. 2014, *arXiv:1412.6980*. [Online]. Available: https://arxiv.org/abs/1412.6980

[46] M. H. Ionica and D. Gregg, "The movidius myriad architecture's potential for scientific computing," *IEEE Micro*, vol. 35, no. 1, pp. 6–14, Jan./Feb. 2015.

[47] F. Kaup, P. Gottschling, and D. Hausheer, "Powerpi: Measuring and modeling the power consumption of the raspberry pi," in *Proc. 39th Annu. IEEE Conf. Local Comput. Netw.*, Sep. 2014, pp. 236–243.

Dmitrii Shadrin received the B.S. degree (Hons.) and the M.S. degree in applied physics and mathematics from the Moscow Institute of Physics and Technology (MIPT), Dolgoprudny, Russia, in 2014 and 2016, respectively. He is currently pursuing the Ph.D. degree with the Skolkovo Institute of Science and Technology (Skoltech), Moscow, Russia.

He is also involved in the development of the Precision Agriculture Lab, Skoltech, where he is responsible for the experimental research and a number of projects. His current research interests include data processing, modeling of physical and bio processes in closed artificial growing systems, machine learning, and computer vision.

Alexander Menshchikov received the degree in applied physics and mathematics from the Moscow Institute of Physics and Technology (MIPT), Dolgoprudny, Russia, in 2014. He is currently pursuing the Ph.D. degree in data science with the Skolkovo Institute of Science and Technology (Skoltech), Moscow, Russia.

As a Skoltech M.S. student, he visited the Aeroastro Department, Massachusetts Institute of Technology (MIT), Cambridge, MA, USA, for the spring semester. Before joining Skoltech, he was an Engineer with the Central Aerohydromechanis Institute (TsAGI), Zhukovsky, Russia, from 2011 to 2014, a Space Systems Engineer with Sputnix Company, Russia, and Dauria Aerospace Company, Russia, from 2015 to 2016, an Engineer with the Mechatronics and Robotics Group, TOPCON Company, Russia, from 2017 to 2018. He has ten publications in peer-reviewed international journals and conference proceedings. His current research interests include robotics, artificial intelligence, and embedded systems.

Andrey Somov received the degree and the diploma degree in electronics engineering from MATI-Russian State Technological University, Moscow, Russia, in 2004 and 2006, respectively, and the Ph.D. degree in electronic engineering from the University of Trento, Trento, Italy, in 2009, with a focus on power management in wireless sensor networks (WSNs).

Before joining Skoltech in 2017, he was a Senior Researcher with the CREATE-NET Research Center, Trento, from 2010 to 2015, and a Research Fellow with the University of Exeter, Exeter, U.K., from 2016 to 2017. He is currently an Assistant Professor with the Skolkovo Institute of Science and Technology (Skoltech), Moscow. He has published more than 70 articles in peer-reviewed international journals and conferences. His current research interests include power management for the wireless sensor nodes, cognitive Internet of Things, and associated proof-of-concept implementation.

Dr. Somov holds some awards in the fields of WSN and IoT, including the Google IoT Technology Research Award in 2016 and the Best Paper Award at the IEEE IoP conference in 2019.

Gerhild Bornemann started her career at the University of Bonn, Bonn, Germany, studying biology. She early took interest in the field of evolutionary ecology and specialized in insect mating behavior with special attention to interindividual and species interactions. After finishing her doctorate, she started working in the DLR-project C.R.O.P. Applying her specialist knowledge and experience in the dynamics of natural systems, she developed a theoretical frame, which provides the basis for the design of resilient closed biological systems. She is currently the Head of the C.R.O.P. Biofiltration Laboratory, Cologne, Germany, in which the capability of biofilters to prepare urine and blackwater for reuse in hydroponic greenhouse cultivation is evaluated. In cooperation with colleagues from other disciplines, she develops ideas and projects to integrate wastewater recycling in Life Support Systems for space flights and in modern greenhouse systems like vertical farms.

Jens Hauslage has studied biology and plant physiology from the Institute of Gravitational Biology, University of Bonn, Bonn, Germany, under the supervision of A. Sievers and M. Braun from 1999 to 2005. He received the Ph.D. degree *(Magna cum laude)* from the University of Bonn in 2008.

After his diploma in biology, he got a Ph.D. grant to unravel the functional mechanisms of gravity sensing in plants. As leading PI participates several parabolic plane flight and sounding rocket campaigns with self-developed experimental setups and facilities for using under microgravity. He started to work in the German Aerospace Center, Russia. First time in the development of ground base facilities to produce functional weightlessness for small organisms, cell cultures, and plants. Besides his research activities at the DLR, he gave lecturers at the University of Bonn, University of Hohenheim, Stuttgart, Germany; the International Space University, Strasburg, France; the University of Erlangen, Erlangen, Germany; and the Skolkovo Institute of Science and Technology, Moscow, Russia.

Dr. Hauslage was an Editor of the *Journal Microgravity, Science and Technology* and an Active Reviewer of *Acta Astronautica*, *Reach*, *Microgravity Science and Technology*, and the *Life Science for Space Research*.

Maxim Fedorov received the Ph.D. degree in physics and mathematics and the D.Sc. degree in physical chemistry from the Russian Academy of Sciences, Moscow, Russia, in 2002 and 2007, respectively.

He is currently a Professor and the Director of the Skoltech Center for Computational and Data-Intensive Science and Engineering (CDISE), Moscow. He has significant experience in coordinating international projects in scientific computing, applications of modeling techniques to real-world tasks, and development of sustainable large-scale e-infrastructure for computational science and engineering. His track-record includes other appointments in leading international research and academic organizations, such as a Full Professorship (Chair) in physics with the Department of Physics, University of Strathclyde, Glasgow, U.K.; the Research Group Leader of the Max Planck Institute for Mathematics in the Sciences, Leipzig, Germany. He holds research positions at different levels with the Institute of Theoretical and Experimental Biophysics (Pushchino Biological Centre of RAS), Russia, National Research Centre "Kurchatovskyi Institut," Moscow; University College Dublin, Dublin, Ireland; and the Unilever Centre for Molecular Science Informatics, Chemistry Department, University of Cambridge, Cambridge, U.K.